

Experimental study of pressure rise at the evaporator of capillary pumped loop with acetone and water as working fluids

Paweł Szymański^a, Dariusz Mikielwicz^b

^a Faculty of Ocean Engineering and Ship Technology, Gdansk University of Technology, Poland

^b Faculty of Mechanical Engineering, Gdansk University of Technology, Poland

Abstract

In this work studied is the possibility of fluid pumping using capillary forces in the capillary pumped loop. Experimental and theoretical studies have been performed to understand the phenomena associated with heat transfer in porous structure of the evaporator. The capillary effect was studied during operation of two different capillary porous structures with two different working fluids, namely water and acetone. The results gave a foundation for a new concept of modern evaporator for waste heat recovery that supports the fluid pumping in the thermodynamic cycle. The results shows that evaporator filled by capillary wick made of Ni-Cu sintered porous material can produce the pressure difference up to 1.63 kPa at the heat rate input of 100 W.

Keywords: Loop Heat Pipe, Capillary Pumped Loop, Porous media, Multiphase flow, Heat transfer

1. Introduction

Applications utilizing cogeneration and recovery of waste heat are a promising new direction of modern dispersed energy sector development. One such example that could, in the future, supplement the centralized energy sector is the micro-CHP combined heat and power unit (micro-CHP) operating according to the Clausius–Rankine cycle. In such installations usually other than water fluids are used, namely the low-boiling point fluids. In case of implementation of the latter fluids there arises a problem of excessive demand for pumping power. Using capillary forces for pumping working fluid in the organic Clausius–Rankine (ORC) is a new idea that allows for reduction or even elimination of the pumping device the working fluid in such cycles. Evaporator filled by porous material that pumps the working fluid in the system, could also be used for other industrial applications where ORC can be used, such as or example micro-CHP heat and power plants for single households, refrigeration and air conditioning systems etc. The use of capillary forces will reduce the pumping power required for circulating pump operating in a thermodynamic cycle (which in case of low-boiling fluids is significant), thus reducing power consumption, which gets the circulating pump, and consequently reduce CO₂ emissions and limit the environment degradation.

There are typically two types of capillary action aided devices. A two-phase pump loop with porous structure, namely the Loop Heat Pipe (LHP), is an efficient heat transfer system based on the liquid-vapor phase change phenomena. The device consists of an evaporator, condenser, compensation chamber and finally the vapor and liquid transport lines. Only the evaporator and eventually the compensation chamber contain wicks, while the other components could be made of smooth tubing. A two phase capillary loop uses capillary action to circulate the working fluid in a sealed enclosure. Another two-phase capillary pump loop, named Capillary Pumped Loop (CPL), has similar advantages as LHP compared to heat pipe. The basic distinction between a traditional CPL and a traditional LHP lies in the fluidic and thermal attachment of the compensation chamber to the evaporator.

Although conventional capillary pumped loop technology has been successfully applied in the last thirty years for the thermal management of a variety of applications like space applications, electronic cooling and high power devices cooling, to cite a few [1–10]. Using capillary forces in evaporator for pumping a working fluid in thermodynamic cycle (eg. ORC) is a new idea, that allows to reduce or even eliminate the device that pumping working fluid in such cycle. Application and principle of operation of such evaporator was presented by the authors in previous works [11,12].

Evaporator in the CPL serves three functions: (1) to prevent the reflow of vapor into liquid inlet, (2) to pump the working fluid from the condenser to the evaporator to form natural circulation, (3) to

Nomenclature

A	cross-sectional area (m^2)
d	diameter (m)
h_{lv}	latent heat of vaporization (kJ/kg)
L	length (m)
\dot{m}	mass flow rate (g/s)
p	pressure (Pa)
Q	heat load applied to evaporator (W)
r	radius (m)
Re	Reynolds number

Greek symbols

v	velocity (m/s)
ρ	density (kg/m^3)
κ	permeability of the wick (m^2)
ε	wick porosity (%)
σ	surface tension (N/m)
μ	dynamic viscosity (Pa s)

Subscripts

<i>bayonet</i>	bayonet
<i>cap,max</i>	maximum capillary pressure
<i>cc</i>	compensation chamber
<i>cond</i>	condenser
<i>evap</i>	evaporator
<i>grooves</i>	vapor grooves
<i>l</i>	liquid
<i>ll</i>	liquid line
<i>in</i>	internal radius of the wick
<i>out</i>	external radius of the wick
<i>p</i>	pore
<i>wick</i>	wick
<i>v</i>	vapor
<i>vl</i>	vapor line

provide the working fluid a flow path from the evaporator to condenser.

In this work studied the possibility of pumping fluid using a capillary forces in CPL evaporator. The potential application of such a heat exchanger is for example an evaporator of the domestic micro-CHP unit.

2. Experimental design

A CPL with exchangeable evaporator was manufactured and tested in order to evaluate its thermal performance and possible capillary pressure difference created by the evaporator. The pressure rise at the evaporator was measured while the thermal load was varied. In this study tested were two evaporators filled by two different wick materials in cooperation with two different working fluids, namely water and acetone. **The first evaporator** consists of a cylindrical tube filled with the sintered porous wick made of the mixture of nickel and aluminum. This sinter is fully permeable, the pore size radius is $2,5 \mu\text{m}$, permeability is around $5,42 \times 10^{-13} \text{m}^2$, and porosity is 55%. **The second evaporator** is filled by a porous wick made by a sinter of nickel copper powders. This material is also fully permeable, the pore size radius is $2,5 \mu\text{m}$, permeability is $5,88 \times 10^{-13} \text{m}^2$ and the porosity is 60%. Both evaporators have the same construction and both have 10 vapor grooves of $1,7 \text{mm}$ diameter each. In the above mentioned evaporators, vapor channels are located at the surface of the evaporator housing and have been drilled within the porous structure. The geometrical dimensions of the evaporators are shown in Fig. 1 and the appearance is presented in Fig. 2.



Fig. 2. Evaporator filled with a wick. Ni-Cu (left side) and Ni-Al (right side).

The evaporator housing is made of stainless steel with a wall thickness of 1mm . This material was used because of the possibility of testing various liquids to eliminate any destruction (corrosion) of the casing material through testing an incompatible fluids.

For the heating of the capillary evaporator, electrical resistant wire of heating power of 100W was wound around wick section of evaporator casing and connected to laboratory DC supplier with adjustable voltage and current. The electric power applied to the electric resistor was calculated by measuring the current and voltage across it. Assuming no heat losses through the insulation in the heating zone, the applied electrical power is taken as the rate heat

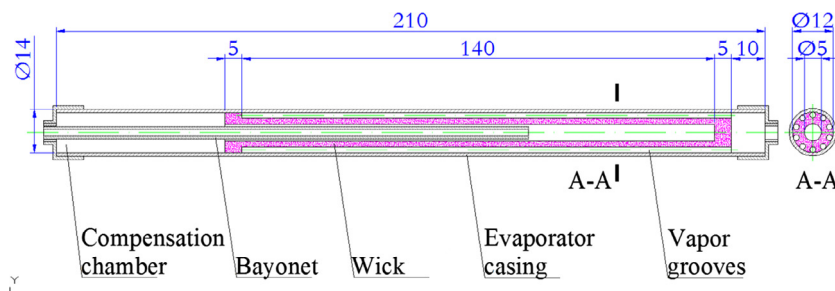


Fig. 1. The outline of evaporator with relevant dimensions (in scale).



applied to the system. A simple heat transfer analysis provided that the heat loss from the heating cartridge to the external ambient amounted in steady state, to less than 2% of the applied heat load.

The condenser of CPL was a typical double pipe heat exchanger, where the inner tube diameter is 3.87 mm and a wall thickness is 1.24 mm, external tube diameter is 14 mm and a wall thickness is 1.5 mm. Condenser was cooled by means of the tap water with adjustable flow rate (rotameter). Cooling of the condenser was adjusted to keep the system pressure constant.

One of the most important and most difficult to design element of capillary pumped loop is the reservoir which is responsible for hydrodynamic control of the loop and regulation of temperature and pressure in the system. The reservoir must be constructed so that the maximum operating temperature of the CPL could compensate the thermal expansion of the working fluid (operating conditions at the lowest temperature to the most difficult conditions in the highest operating temperature). The reservoir dimensions were chosen experimentally by trial and error method and its final volume was set to 0.5 dm³. The reservoir was connected to the loop by the tube with an internal diameter of 3.87 mm. Another heat source necessary for triggering the CPL operation is a heater located on the reservoir outer wall. For this purpose Watlow's flexible silicone heating mat of maximum heating power of 300 W was used powered by DC laboratory power supplier with adjustable voltage and current. The advantage of the flexible heating mat is its ability to adjustment to the arbitrary shape, which provides a good fit to the heated surface, and thus better thermal contact. The heating mat was responsible for the constant heating and maintaining a steady temperature (and pressure) in the reservoir of the capillary pumped loop.

The liquid and vapor lines are made of acid resistant stainless steel tubes with inner diameters of 3.87 mm and length of 50 mm.

Fig. 3 presents a schematic of the experimental setup for testing capillary pump loop and Fig. 4 shows the general view of the facility.

The performance tests were carried out for various power inputs ranging from 20 to 100 W for evaporator filled by a Ni-Cu porous wick and water as a working fluid and for evaporator filled by Ni-Al porous wick and acetone as a working fluid. The evaporator filled by a Ni-Cu porous wick and acetone as a working fluid was tested only for power inputs up to 50 W. Evaporator filled by a Ni-Al porous wick has not been tested with the water as a working fluid, because water is not recommended as the working fluid in the system, where one of the construction material is aluminum [13].

The test set up for testing the pressure rise in the CPL evaporators consists the following measurements:

- Absolute pressure inside the loop – pressure transducer to measure the absolute pressure inside the loop installed on the liquid line (pressure transducer **P1** shown in Fig. 3).
- Pressure difference – transducer measuring the pressure difference between evaporator inlet and outlet. This transducer was connected to the loop via a tube with diameter of 3.87 mm. The differential pressure measurement is one of the most important measurement in this study (differential pressure transducer **P2** shown in Fig. 3).
- Evaporator casing temperature - thermocouple “type T” measuring a range of temperature from –200 °C to +350 °C and sensitivity of 30 μV/K (thermocouple **T3** shown in Fig. 3).

The working fluid, must operate without impurities as an important condition to avoid the appearance of non-condensable gases (NCG) in the loop. The presence of NCG in CPL can cause a failure in capillary evaporator, but as the CPL is initially evacuated

from air it is less prone to occur in closed circuits. Ensuring a good vacuum seal in the loop as well as using fluid with a minimum amount of contaminants also minimizes the presence of NCGs. Before start of the experiment, the non-condensable gas embedded in the device of system and reservoir was eliminated using a vacuum pump to prevent residual NCG from impeding flow and prompting the deprime issue. Due to the non-condensable nature of the gas, the pressure of the system device was drawn out using a two-step rotary vane vacuum pump (model VALUE Vi220SV) to maintain a low pressure of around $1.5 \cdot 10^{-4}$ kPa.

The uncertainties were calculated for temperatures, pressure drop in evaporator, and heat transfer rates, which are given by

$$U_Y = \sqrt{\sum_i \left(\frac{\partial Y}{\partial X_i}\right)^2 U_X^2} \quad (1)$$

where X_i and Y represent measured and calculated variables, respectively. U_X and U_Y are the measured and calculated uncertainties, respectively.

3. Experimental procedure

3.1. Capillary limit analysis of the CPL

The main operational limits of capillary pumping loop is the boiling and capillary limits. In this section, the capillary limit will be explored based on an analysis of the experimental results. The condition under which CPL operate is that the total system pressure drop does not exceed the maximum pressure that the porous wick can provide. Due to the vapor penetration through the porous wick, the operating temperature of the system has a sudden increase when the capillary limit is exceeded. Thus, the capillary pumping system operation requires that the sum of the pressure drops in the components and in the transport lines must be smaller than the maximum capillary pressure head developed by the wick, i.e.,

$$\Delta p_{cap,max} = \frac{2\sigma}{r_p} \geq \Delta p_{evap} + \Delta p_{cond} + \Delta p_{vl} + \Delta p_{ll} \quad (2)$$

The maximal capillary pressure was measured to be 1.76 kPa based on the bubble point measurement using acetone as a wetting fluid that measures how much pressure the membrane can handle before pressurized gas pass through it. This value also helps to characterize the porous membrane by giving an estimation of the average pore radius to be 2.5 μm and permeability of the wick, that can be calculates as,

$$\kappa_{wick} = \frac{4r_p^2 \varepsilon^3}{150 \cdot (1 - \varepsilon)^2} \quad (3)$$

where ε is porosity.

3.2. Single-phase pressure drop

In the following study it was assumed that the single phase flow prevail along the grooves, vapor and liquid lines, and in the porous wick. It was also assumed that half of the condenser line was liquid phase and half a vapor phase. The single phase pressure drop can be estimated from the Darcy-Weisbach equation,

$$\Delta p = f \left(\frac{L}{d}\right) \left(\frac{\rho v^2}{2}\right) = f \left(\frac{L}{d}\right) \left(\frac{\dot{m}^2 A^2}{2\rho}\right) \quad (4)$$

where f is the Darcy friction factor. When the laminar flow occurs in circular tubes then $fRe = 64$. For turbulent flow in smooth tubes f

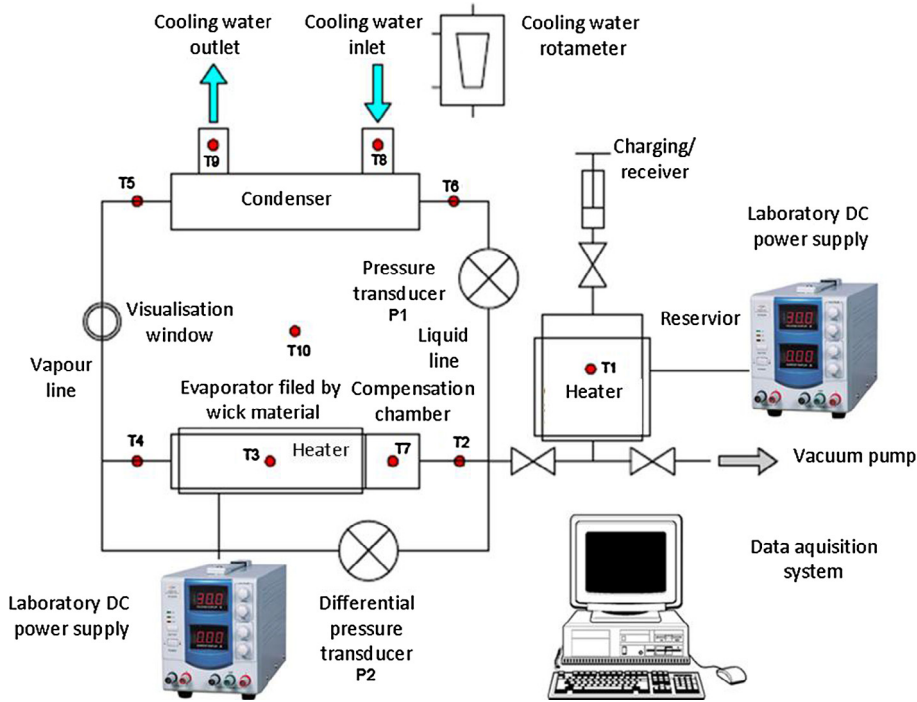


Fig. 3. Schematic of experimental setup for testing capillary pump loop.

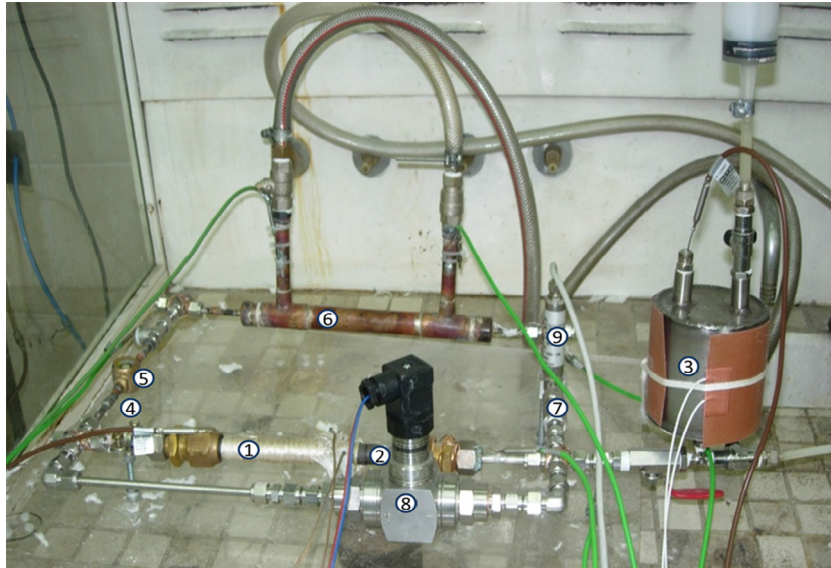


Fig. 4. View of test facility (before insulation). 1 – Evaporator. 2 – Compensation chamber. 3 – Reservoir. 4 – Vapor line. 5 – Visualisation window. 6 – Condenser. 7 – Liquid line. 8 – Differential pressure transducer. 9 – Pressure transducer.

was estimated from equation proposed by H. Blasius, $f = 0.316Re^{-0.25}$ for $4000 < Re < 10^5$.

The liquid velocity through the porous wick, according to Darcy's law, can be written as,

$$v_{wick,l} = -\frac{\kappa_{wick}}{\mu_l} \frac{dp}{dr} \quad (5)$$

or

$$\dot{m}_l = \rho_l v_{wick,l} A_{wick} = -\frac{\rho_l 2\pi r L_{wick} \kappa_{wick}}{\mu_l} \frac{dp}{dr} \quad (6)$$

where ρ_l is the liquid density, $v_{wick,l}$ is the Darcy liquid velocity within the wick, A_{wick} is the cylinder wall area of the wick, κ_{wick} is the saturated permeability and L_{wick} is the length of the wick.

Integrating Eq. (6) from $r_{wick,in}$ to $r_{wick,out}$, assuming \dot{m}_l , μ_l and κ_{wick} are constants, the pressure drop in the porous wick can be calculated from,

$$\Delta p_{wick} = \frac{\dot{m}_l \mu_l}{2\pi \rho_l \kappa_{wick}} \ln \left(\frac{r_{wick,out}}{r_{wick,in}} \right) \quad (7)$$

Using equations (2)–(7) the total pressure drop of the system, which enables determination of the mass flow rate from the implicit equation:

$$\begin{aligned} \Delta p = & f_{cc} \left(\frac{L_{cc}}{d_{cc}} \right) \left(\frac{\dot{m}^2 A_{cc}^2}{2\rho_l} \right) + f_{bayonet} \left(\frac{L_{bayonet}}{d_{bayonet}} \right) \left(\frac{\dot{m}^2 A_{bayonet}^2}{2\rho_l} \right) \\ & + \frac{\dot{m} \mu_l}{2\pi \rho_l K_{wick} L_{wick}} \ln \left(\frac{r_{wick,out}}{r_{wick,in}} \right) \\ & + f_{grooves} \left(\frac{L_{grooves}}{d_{grooves}} \right) \left(\frac{\dot{m}^2 A_{grooves}^2}{2\rho_v} \right) + f_{vl} \left(\frac{L_{vl}}{d_{vl}} \right) \left(\frac{\dot{m}^2 A_{vl}^2}{2\rho_v} \right) \\ & + f_{cond} \left(\frac{L_{cond}}{d_{cond}} \right) \left(\frac{\dot{m}^2 A_{cond}^2}{2\rho_l} \right) + f_{ll} \left(\frac{L_{ll}}{d_{ll}} \right) \left(\frac{\dot{m}^2 A_{ll}^2}{2\rho_l} \right) \end{aligned} \quad (8)$$

The mass flow rate through the evaporator can also be estimated using latent heat of vaporization and the heat load that has been applied to evaporator by the heater:

$$\dot{m} = \frac{\dot{Q}}{h_{lv}} \quad (9)$$

The calculations and fluid properties considered in the present model to estimate the pressure drop in the capillary pumped loop were obtained from the software F-Chart Engineering Equation Solver (ver. 8.116) These properties include latent heat of vaporization, saturation pressure, liquid and vapor densities, liquid and vapor viscosities, liquid and vapor thermal conductivities, liquid and vapor specific heats and liquid surface tension.

4. Results and discussion

As mentioned before, experiments were performed for two evaporators in operation with two different working fluids under various thermal loads. In this study was recorded the pressure difference before and after the evaporator, in order to measure the pressure rise generated by the evaporator with a porous wick. Another measurement performed in the experiment was the absolute pressure inside the loop. The pressure measurement is necessary to determine the saturation temperature of the working fluid

contained in the system. The results for the system with water as a working fluid are shown in Fig. 5, while the results for the of acetone are shown in Figs. 6 and 7.

4.1. Pressure rise tests for CPL with water as a working fluid

The test of the CPL with water as a working fluid took 12 h, where the first 3 h was a system preparation (reservoir heating) in order to obtain a steady state and constant temperature in the loop. After 3 h of heating, the temperature inside the reservoir reached about 120 °C. Once obtained the steady state inside the system, started heating up the evaporator at low power, *ie.* 20 W.

The absolute pressure in the system was measured by the pressure transducer installed on the liquid line. The pressure was constant during operation of the system (*ie.* from the start-up) and it was 324 kPa. Inside the loop occurred saturation state, which at the above pressure, corresponded to temperature of 136.2 °C.

Start-up of the system (working fluid flow) was determined at the visualization window installed on the vapor line and at the differential pressure transducer.

Evaporator temperature was measured on the outer wall of the evaporator, and the thermocouple was placed under the heater. The temperature rise was followed sequentially in accordance with supplied increase of heat input. Initial heat supplied to evaporator was 20 W, then its value increased by 10 W every 1 h, to achieve a power of 100 W. After applying such power, the evaporator temperature set at approx. 230 °C.

The analysis of the pressure drop in the system was carried out by measuring the heat load applied, the temperature of the evaporator wall and their influence on the pressure difference before and after the evaporator.

As shown in Fig. 5, the pressure drops in the CPL are not constant even in a seemingly stable operation and exhibit an oscillatory behavior. Pressure oscillations in CPL are normally occurring

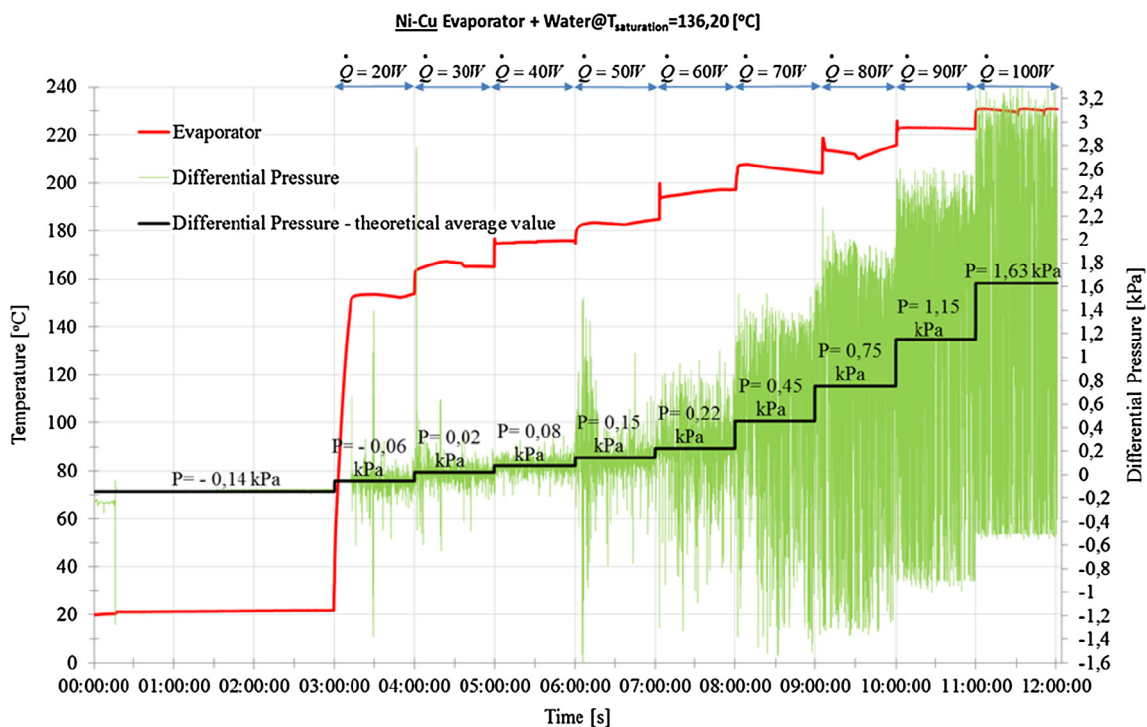


Fig. 5. Effect of heat load on the temperature distribution and the pressure difference for evaporator filled by wick made by Ni-Cu material in cooperation with water as the working fluid.

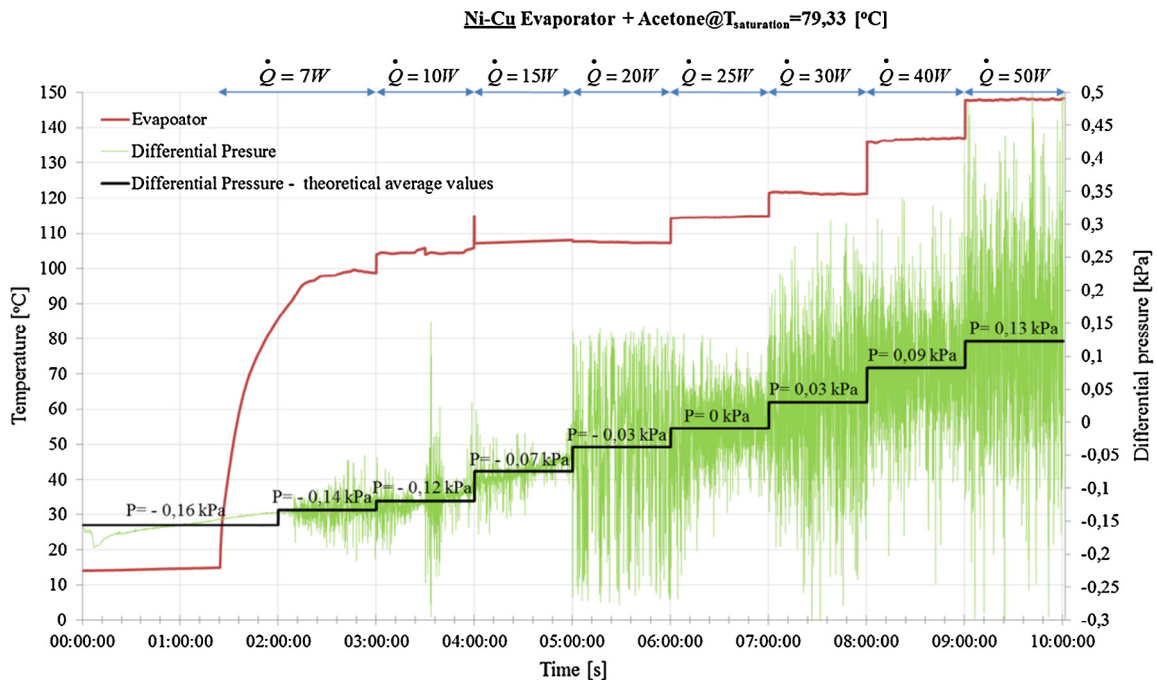


Fig. 6. Effect of heat load on the temperature distribution and the pressure difference for evaporator filled by wick made by Ni-Cu material in cooperation with acetone as the working fluid.

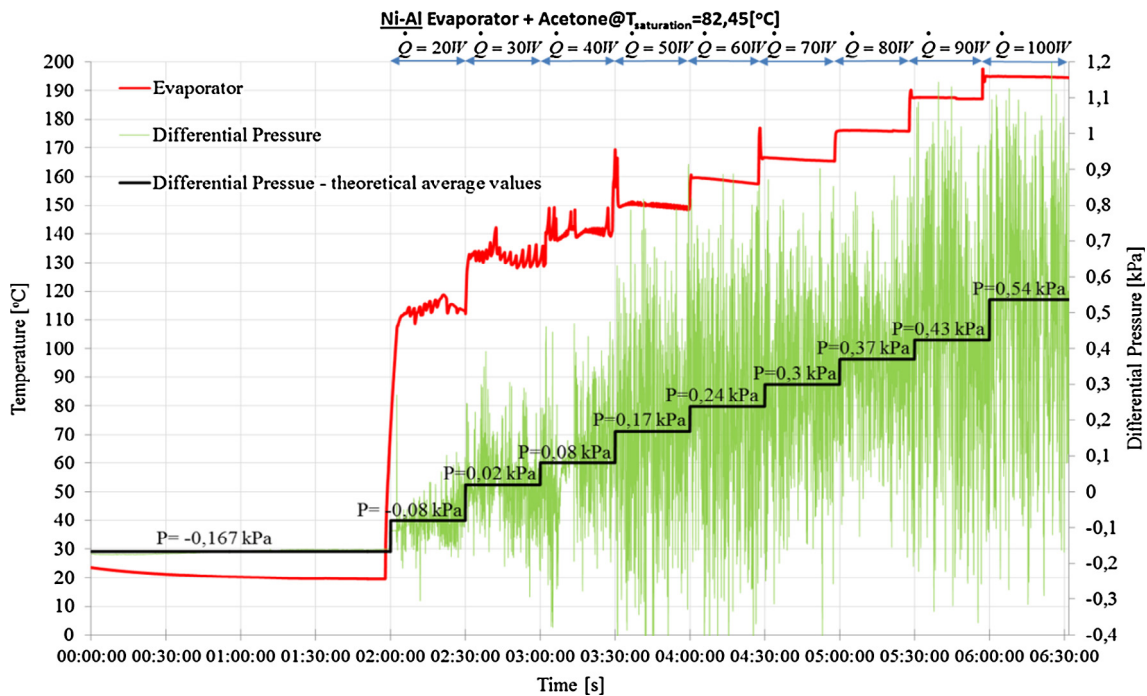


Fig. 7. Effect of heat load on the temperature distribution and the pressure difference for evaporator filled by wick made by Ni-Al material in cooperation with acetone as the working fluid.

process and result from hydrodynamic instability between evaporator filled by porous wick and reservoir.

Ku and Hoang [14] suggest that pressure oscillations have no negative impact on the CPL operation nevertheless during the tests there were several unexplained anomaly that may be associated with the pressure oscillations (eg. system deprim).

The frequency and amplitude of the pressure oscillations are the function of the physical dimensions of the CPL elements such as

the dimensions of transport lines and working conditions (eg. heat load applied to the system and the temperature in the evaporator and condenser). Pressure oscillations are affected by: the mass flow rate in the loop, pressure drops in the system, the dimensions of the vapor line, volume of the reservoir and dimensions of the line connecting the reservoir and the loop.

At the beginning of the measurement (ie. during system preparation – reservoir heating up), the initial indication of differential



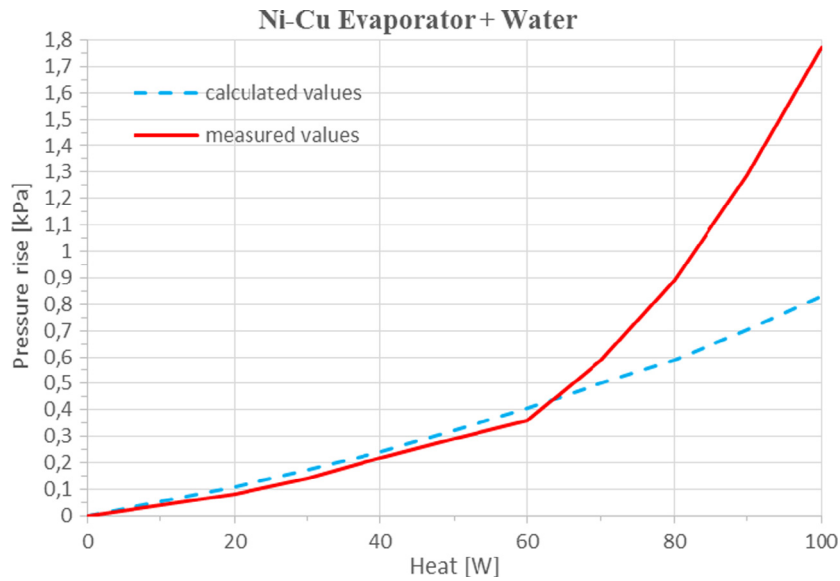


Fig. 8. Effect of heat load on the pressure difference for Ni-Cu wick evaporator and water as a working fluid – comparison between values obtained at the experiment and values calculated by the mathematical model.

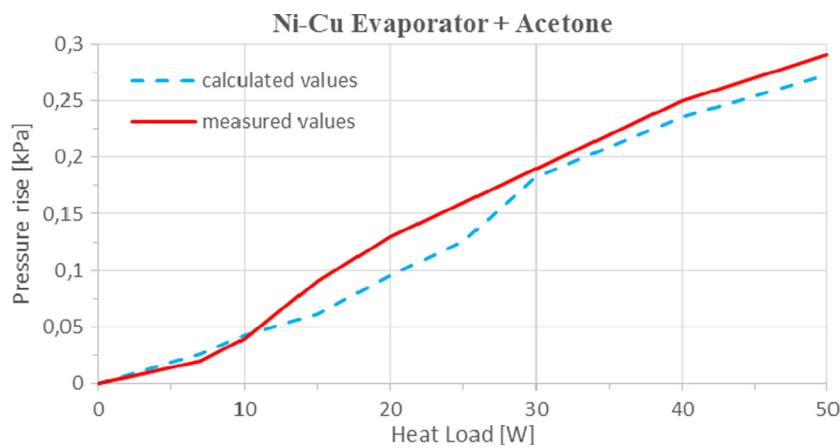


Fig. 9. Effect of heat load on the pressure difference for Ni-Cu wick evaporator and acetone as a working fluid – comparison between values obtained at the experiment and values calculated by the mathematical model.

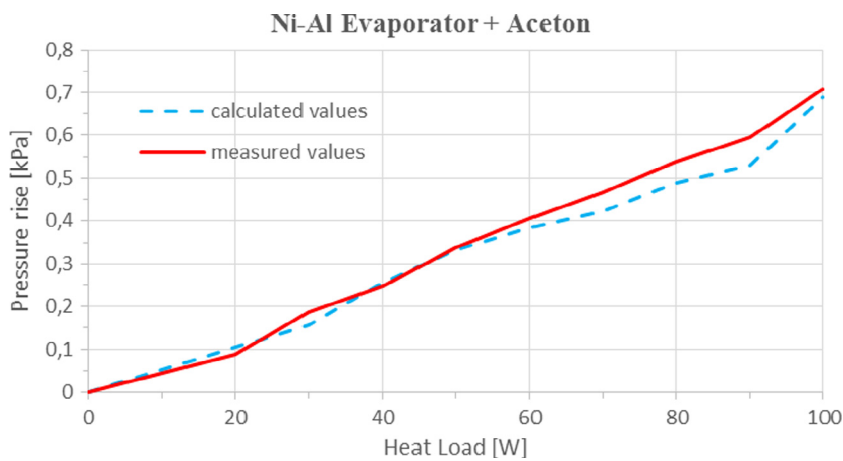


Fig. 10. Effect of heat load on the pressure difference for Ni-Al wick evaporator and acetone as a working fluid – comparison between values obtained at the experiment and values calculated by the mathematical model.

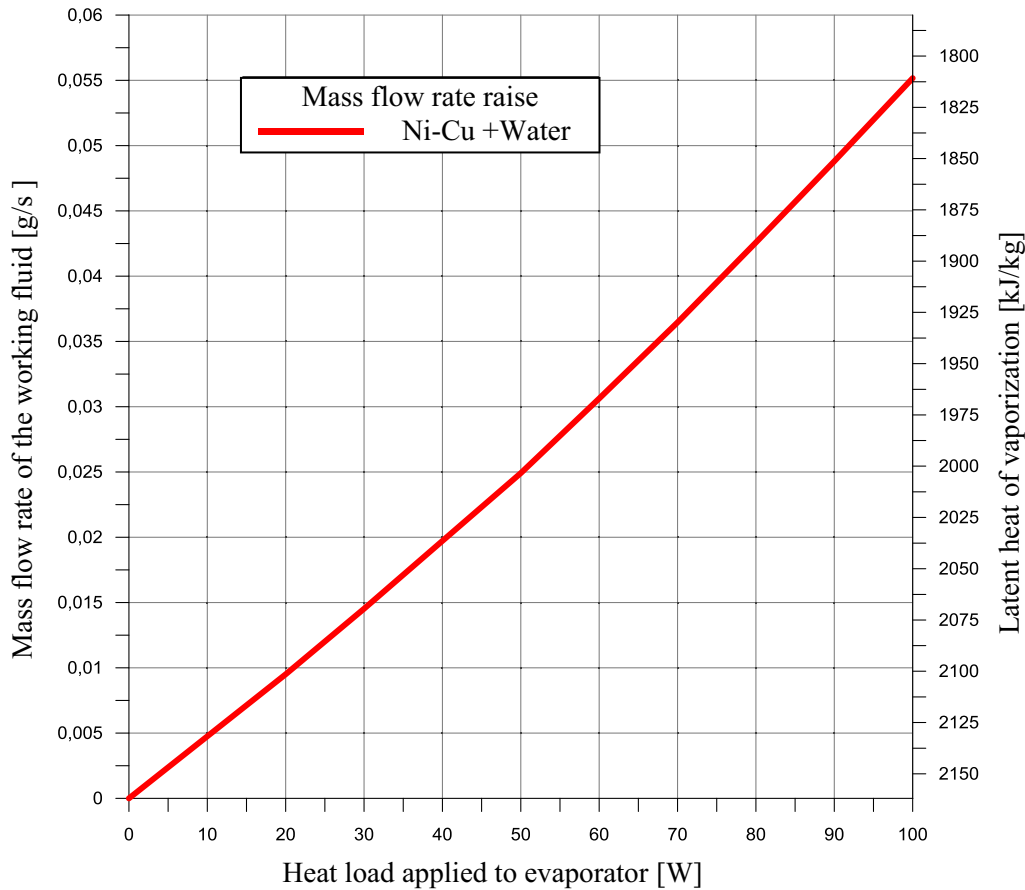


Fig. 11. Effect of heat load on mass flow rate for Ni-Cu evaporator with water as the working fluid.

pressure transducer was -0.14 kPa. Despite the lack of fluid flow inside the loop, the pressure difference indication was “negative”, because the working fluid located in the reservoir caused the pressure on “negative side” of the differential pressure transducer.

In a result of applying to evaporator a heat load of 20 W, fluid flow was observed at the visualization window and the differential pressure transducer indicated an increase in pressure difference inside the system. In the initial setting of the heater, the amplitude of pressure oscillations was low and amounted to approx. 0.15 kPa (ie. from -0.24 kPa to 0.09 kPa), so that the pressure difference has increased to an average level of -0.06 kPa, which corresponds to total pressure difference at approx. 0.2 kPa.

In this test the heat load applied to the system was increased, after determining the steady state, every hour of 10 W. This corresponded to a stepwise growth of pressure difference and increasing oscillation to this parameter. In the final setting of the heater, ie. 100 W, the pressure difference in the system was approx. 1.8 kPa, and the amplitude of the pressure oscillations 3.6 kPa.

4.2. Pressure rise tests for CPL with acetone as a working fluid

The second working fluid analyzed in this study was pure acetone, which was tested in CPL with two different evaporators i.e. evaporator filled by Ni-Cu wick and evaporator filled by Ni-Al wick. Acetone is a working fluid commonly used in CPL and LHP systems and is chemically compatible with materials used for production of evaporators and porous wick, moreover, it is characterized by high commercial availability and low boiling point.

CPL with Ni-Al porous wick was prepared to work (heated up) for 2 h and the whole measurement cycle took 6.5 h. Preparation

time selected individually by “trial and error” method for each installation so that, in contrast to the previous test (CPL Ni-Cu wick and water as a working fluid), this time has been shortened by an hour to shorten the total time of measurement session. For the first two hours reservoir was heated by a constant heat until its temperature stabilized at about 80 °C and the pressure inside the loop reached a value of approx. 230 kPa (which corresponds to a saturation temperature of acetone at 80 °C). According to Tomlinson [15], in typical CPL installations with acetone as a working fluid the temperature inside the reservoir must be stabilized at about 80 °C. Then it is possible to apply heat load to evaporator. Installation with Ni-Cu porous wick was prepared to work for 1.5 h and the entire measurement session took 10 h. As mentioned earlier, for each installation time preparation time can might be different and is determined experimentally.

CPL with Ni-Al wick was heated initially by 20 W and the heat load was increased stepwise of 10 W every half an hour, until it reached maximum power of 100 W. CPL with Ni-Cu wick initially was heated by 7 W and the heat load was increased stepwise of 5 W by an hour, until it reached maximum power of 50 W. The maximum heating power in this installation is different from the other because the system was equipped with different laboratory power supplier with a maximum power of 50 W. As shown in Fig. 7 the startup of installation (fluid flow) was observed after applying of heat load of 20 W.

Fig. 6 shows the effect of heat load on the temperature distribution and the pressure difference for evaporator filled by Ni-Cu wick in cooperation with acetone as the working fluid and Fig. 7 shows the effect of heat load on the temperature distribution and the pressure difference for evaporator filled by Ni-Al wick in coopera-

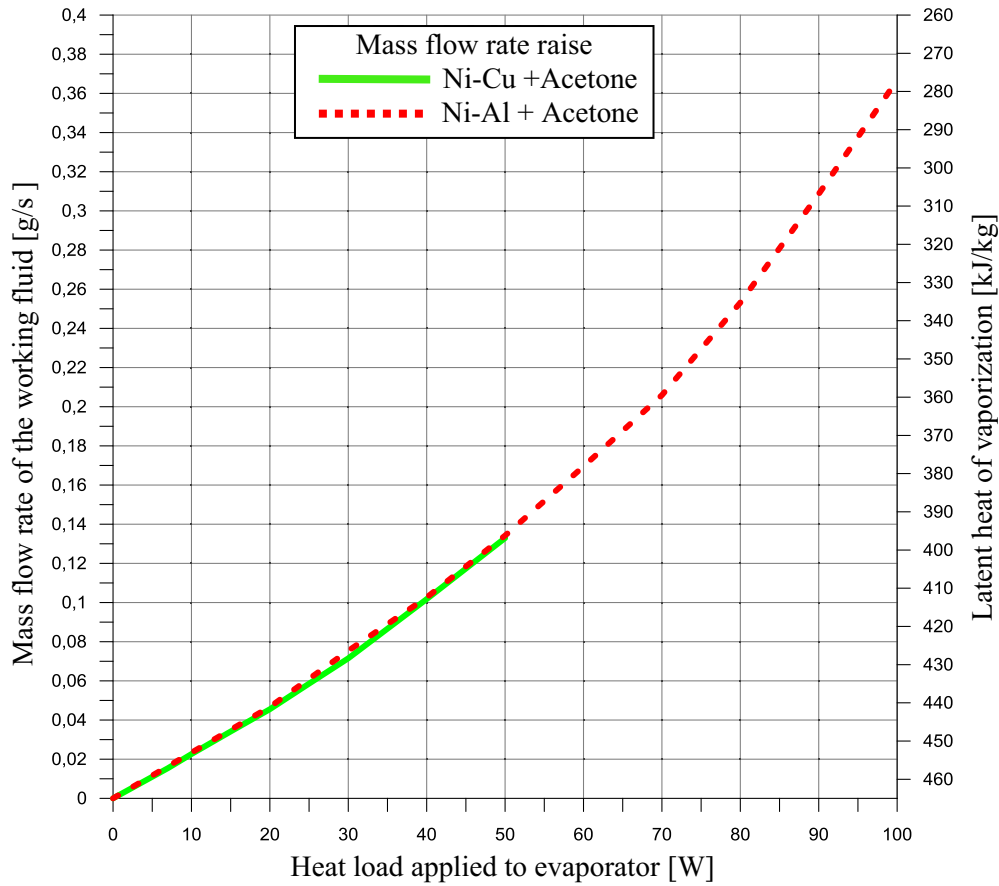


Fig. 12. Effect of heat load on mass flow rate for Ni-Cu evaporator and Ni-Al evaporator with acetone as the working fluid.

tion with acetone as the working fluid. The initial pressure difference (before applying the heat load to evaporator) was -0.16 kPa at the installation with evaporator filled by Ni-Cu wick and -0.167 kPa at the installation with evaporator filled by Ni-Al wick.

Taking into account the accuracy of the measurement equipment, various external conditions during the test and small differences between these values, it can be considered that the initial pressure difference at the start of measurements for two evaporators was the same.

At the end of the measurement (at 100 W) in the system with a Ni-Al wick differential pressure increased by 0.7 kPa, and the amplitude of the oscillations was approx. 1.2 kPa. In the Ni-Cu wick evaporator at the end of the measurement series (at 50 W) differential pressure increased by 0.3 kPa, and the amplitude of oscillations was 0.5 kPa. For 50 W heat load in the two evaporators differential pressure value was similar and the difference between them was in the range of measuring error of differential pressure transducer.

Fig. 8 shows that at the CPL with evaporator filled by Ni-Cu wick and water as a working fluid, at the heat load of 100 W maximum pressure difference is 1.7 kPa, while at the same parameters values calculated from the mathematical model is 0.83 kPa.

The values obtained from the mathematical model the measured are comparable for heating power heater up to 70 W.

For larger heating power supplied to the evaporator we have to deal with a two-phase flow inside the installation. In this case, the flow resistance should be determined based on the so called "two-phase multiplier". For small vapor content in the fluid flow the value multiplier is usually in the range of 2–4. Taking this into account in the calculations would lead to better consistency between calculations and experimental measurements. The local

two-phase flow multiplier can be evaluated in accordance to the assumed flow model. From amongst existing in literature correlations the models due to Martinelli-Nelson, Chisholm, Friedel, Muller-Steinhagen and Heck and homogeneous model are advised to be used in calculations [16].

In the case of CPL with Ni-Cu wick evaporator and acetone as a working fluid, the maximum differential pressure value (for 50 W) obtained at the experiment is 0.28 kPa, while at the same heating power differential pressure value calculated from the mathematical model is 0.26 kPa. Considering accuracy of differential pressure transducer used to measure the pressure increase in the installation (± 0.05 kPa) in this case mathematical model accurately reflects the values of obtained at the experiment (see Fig. 9).

For installation with an evaporator with a porous filling material Ni-Al and acetone as a working fluid the maximum pressure value (at heater power of 100 W) is 0.7 kPa, which is similar to the value calculated from the mathematical model (see Fig. 10).

4.3. Calculation of mass flow rate of working fluid in the CPL

During the tests the important information is a flow rate of working fluid within the system. In the case of CPL this task is very difficult. The procedure applied in the present study was executed in the steady state conditions, where based on the knowledge of the heat load supplied to the evaporator and the latent heat of vaporization of working fluid determined was the mass flow rate of the working fluid in the CPL on the basis of heat balance.

Fig. 11 presents the mass flow rate distribution for the CPL with water as a working fluid whereas Fig. 12 presents the mass flow rate distribution for CPL with acetone as a working fluid.

As shown in the above Figures the maximum flow rate achievable in CPL with water as working fluid is 0.055 g/s whereas in CPL with acetone as the working fluid it is 0.37 g/s.

5. Conclusions

In the paper presented are the experimental results of maximal pressure rise created by evaporator filled by the capillary wick. Two evaporators filled by the two different capillary wicks have been tested in operation with two different working fluids (water and acetone) at the various heat load applied to evaporators.

The passive device (no moving parts) has been presented in the paper that can aid the operation of the circulation pump in the thermodynamic cycle. At the moment the presented pumping effect is not too significant but nevertheless present. The whole idea of capillary pumping arose from the fact that the domestic micro-CHP requires a high level of pumping power, which results in very expensive devices. The proposed principle of operation can be implemented to aid the circulation of working fluid. The example of application would be the domestic micro-CHP, which has been presented in some detail in [17].

References

- [1] Y. Tang, J. Xiang, Z. Wan, W. Zhou, L. Wu, A novel miniaturized loop heat pipe, *Appl. Therm. Eng.* 30 (10) (2010) 1152–1158.
- [2] P.C. Chen, W.K. Lin, The application of capillary pumped loop for cooling of electronic components, *Appl. Therm. Eng.* 21 (17) (2001) 1739–1754.
- [3] M. Crepinsek, C. Park, Experimental analysis of pump-assisted and capillary-driven dual-evaporators two-phase cooling loop, *Appl. Therm. Eng.* 38 (2012) 133–142.
- [4] P.H.D. Santos, E. Bazzo, A.A.M. Oliveira, Thermal performance and capillary limit of a ceramic wick applied to LHP and CPL, *Appl. Therm. Eng.* 41 (2012) 92–103.
- [5] C.T. Wang, T.S. Leu, T.M. Lai, Micro capillary pumped loop system for a cooling high power device, *Exp. Therm. Fluid Sci.* 32 (2008) 1090–1095.
- [6] D. Butler, J. Ku, T. Swanson, Loop heat pipes and capillary pumped loops—an applications perspective, *AIP Conf. Proc.* 608 (1) (2002) 49.
- [7] Y. Maidanik, Y. Fershtater, V. Pastukhov, Design and investigation of a capillary pumped loop for advanced thermal control systems of space vehicles, *SAE Technical Paper* 951509, 1995.
- [8] X.M. Huang, W. Liu, A. Nakayama, S.W. Peng, Modeling for heat and mass transfer with phase change in porous wick of CPL evaporator, *Heat Mass Transf.* 41 (7) (2005) 667–673.
- [9] D. Liepmann, Design and fabrication of a micro-cpl for chip-level cooling, in: *Proceedings of: 2001 ASME International Mechanical Engineering Congress and Exposition* November 11–16, New York, NY, 2001, 2001.
- [10] D. Mikielewicz, P. Szymanski, Capillary pumped loop as a tool for collecting large heat fluxes from electronic devices on warships, *Polish Maritime Res.* 1 (93) (2017) 72–80 (Vol. 24).
- [11] D. Mikielewicz, P. Szymanski, K. Błaściak, J. Wajs, J. Mikielewicz, E. Ihnatowicz, The new concept of capillary forces aided evaporator for application in domestic organic rankine cycle, *Heat Pipe Sci. Technol.* 1 (4) (2010) 359–373.
- [12] D. Mikielewicz, P. Szymański, Rurka ciepła z pętlą obiegową jako urządzenie do odzysku ciepła, *Techn. Chłodnicza i Klimatyzacyjna* (67) (2011) 298–306.
- [13] A. Faghri, *Heat Pipe Science and Technology*, Taylor & Francis Inc. (ISBN 978-1-56032-383-9).
- [14] J. Ku, T.T. Hoang, An experimental study of pressure oscillation and hydrodynamic stability in a capillary pumped loop, in: *Conference: 1995 National Heat Transfer Conference*, Portland, OR (United States), 5–9 August, 1995.
- [15] B.J. Tomlinson Jr., *Steady State Analysis of Capillary Pumped Loop* MSc Thesis, University of Texas at El Paso, May 1997.
- [16] D. Mikielewicz, J. Mikielewicz, A common method for calculation of flow boiling and flow condensation heat transfer coefficients in minichannels with account of nonadiabatic effects, *Heat Transfer Eng.* 32 (13–14) (2011) 1173–1181.
- [17] J. Wajs, D. Mikielewicz, M. Bajor, Z. Kneba, Experimental investigation of domestic micro-CHP based on the gas boiler fitted with ORC module, *Arch. Thermodyn.* 37 (3) (2016) 79–93.

